れた。移植後 2 年時点で 46.7%の生存率が得られた (Biology of blood and Marrow Transplantation, 18: 633-639, 2012)。第 I 相試験の結果、洗浄することなく、骨髄内へ移植することの安全性が確認できたため、引き続いて、有用性を検討する第 II 相試験 (予定症例数 30 例) を、多施設共同試験の形で実施した。第 II 相試験は、兵庫医科大学の他に、成田赤十字病院、川崎医科大学と都立駒込病院が参加施設となったが、予定症例数の登録が既に完了した。現在、観察期間に入っており、移植後 3 年までの観察を行う予定になっている。

D. 考察

Frassoni らの骨髄内臍帯血移植の臨床研究で、生着などに関して有用性が認められたが、Brunstein らの研究では、それが否定的であった。その違いが生じた 1 つ理由として、骨髄内へ投与する volume に関して、前者が 5 ml であったのに対して、後者が 20 ml であったことが挙げられる。小さな骨髄内スペースに、投与される至適 volume が不明であるが、大量の volume の造血細胞を注入すると、骨髄内は血管網の豊富な組織であるので、すぐに骨髄外に出てしまうことが容易に想像される。我々は、Frassoni らに近く、1 か所当り、6 ml の臍帯血を移植した。このことが良好な生着率に結びついた可能性があると考える。

E. 結論

臍帯血を洗浄することなく、骨髄内へ直接移植する、骨髄内臍帯血移植は、安全に施行可能であることが判明した。

F. 健康危険情報

現在までのところ、骨髄内へ移植する際の軽微な骨痛以外に、通常の臍帯血移植と合併症、副作用において変わりはなく、特記すべき有害事象は観察されていない。

G. 研究発表

1. 論文発表

1) Kaida K, Ikegame K, Ikemoto J, Murata R, Irie R, Yoshihara S, Ishii S, Okada M, Inoue T, Tamaki H, Soma T, Fujimori Y, Kai S, Ogawa H. Soluble interleukin-2 receptor level on day 7 as a predictor of graft-versus-host disease after HLA-haploidentical stem cell transplantation using reduced intensity conditioning. International Journal of Hematology, 99: 463-470, 2014.

2) Eguchi R, Fujimori Y, Okada M, Tamaki H, Wakabayashi I, Ogawa H. Recombinant human soluble thrombomodulin attenuates FK506-induced endothelial dysfunction through prevention of Akt inactivation. Experimental Cell

Research, 323: 112-117, 2014.

3) Yamahara K, Harada K, Ohshima M, Ishikane S, Ohnishi S, Tsuda H, Otani K, Taguchi A, Soma T, Ogawa H, Katsuragi S, Yoshimatsu J, Harada-Shiba M, Kangawa K, Ikeda T. Comparison of angiogenic, cyto-protective, and immunosuppressive properties of human amnion- and chorion-derived mesenchymal stem cells. PLos One, 9: e88319, 2014.

4) Nomura S, Ishii K, Maeda Y, Katayama Y, Yagi H, Fujishima N, Ota S, Seki M, Okada M, Ikezoe T, Hayashi K, Fujita S, Satake A, Ito T, Kyo T, Ishida Y, Chiba S, Ogawa H, Tanimoto M, Sawada K. The preventative effects of recombinant thrombomodulin on transplantation-associated coagulopathy after allogeneic hematopoietic stem cell transplantation. Journal of Stem Cell Research & Therapy, 4: 247, 2014.

5) Matsuda I, Okada M, Inoue T, Tokugawa T, Ogawa H, Hirota S. Primary follicular lymphoma of the spleen incidentally found in a patient with alcohol- and hepatitis C-related liver cirrhosis. Int J Clin Exp Pathol. 7: 4484-4488, 2014.

6) Aoki J, Ishiyama K, Taniguchi S, Fukuda T, Ohashi K, Ogawa H, Kanamori H, Eto T, Iwato K, Sakamaki H, Morishima Y, Nagamura T, Atsuta Y, Takami A. Outcome of allogeneic hematopoietic stem cell transplantation for acute myeloid leukemia patients with central nervous system involvement. Biology of Blood and Marrow Transplantation, 20: 2029-2033, 2014.

7) Ueki D, Ikegame K, Kozawa M, Miyamoto J, Mori R, Ogawa H. Risk analysis of falls in patients undergoing allogeneic hematopoietic stem cell transplantation. Clinical Journal of Oncology Nursing, 18: 396-399, 2014.

8) Matsuoka Y, Nakatsuka R, Sumide K, Kawamura H, Takahashi M, Fujioka T, Uemura Y, Asano H, Sasaki Y, Inoue M, Ogawa H, Takahashi T, Hino M, Sonoda Y. Prospectively isolated human bone marrow cell-derived MSCs support primitive human CD34-negative hematopoietic stem cells. Stem Cells, in press.

9) Fuji S, Takano K, Uchida N, Ogawa H, Ohashi K, Eto T, Sakamaki H, Morishima Y, Kato K, Suzuki R, Fukuda T. Pretransplant diabetes mellitus is a risk factor for infection-related mortality, after allogeneic hematopoietic stem cell transplantation. Bone Marrow Transplantation, in press.

10) Konuma T, Ooi J, Uchida N, Ogawa H, Ohashi K, Kanamori H, Aotsuka N, Onishi Y, Yamaguchi H, Kozai Y, Nagamura-Inoue T, Kato K, Suzuki R, Atsuta Y, Kato S, Asano S, Takahashi S. Granulocyte colony-stimulating factor combined regimen in cord blood transplantation for acute myeloid leukemia: a nationwide retrospective analysis in Japan. Haematologica, 99: e264-268, 2014.

2. 学会発表

1. The 19th European Hematology Association 2014.6.12-15, Milan, Italy. Ishiyama K, Miyawaki S, Kitamura K, Suzuki K, Ishikawa J, Ogawa H, Imai K, Naoe T, Chiba S, Miyazaki Y, Hatta Y, Kurokawa M, Ueda Y, Koga D, Sugiyama H, Takaku F. Clinical usefulness of WT1 mRNA expression in bone marrow detected using a new WT1 mRNA assay kit for monitoring acute myeloid leukemia: A comparison with peripheral blood WT1 mRNA expressions.

2. 2015 BMT Tandem Tandem Meetings, 2015.2.11-15, Ikegame K, Kaida K, Ishii S, Yoshihara S, Taniguchi K, Inoue T, Tamaki H, Okada M, Soma T, Ogawa H. Spousal hematopoietic stem cell transplantation for post-transplant relapse/rejection.

3. 2015 BMT Tandem Tandem Meetings, 2015.2.11-15, Ueki S, Tsujitani M, Teranishi Y, Miyamoto J, Mori R, Ogawa H, Ikegame K. Prediction of skin trouble in patients undergoing allogeneic hematopoietic stem cell transplantation using generalized additive model.

4. 2015 BMT Tandem Meetings, 2015. 2.11-15. Tamaki H, Ikegame K, Yoshihara S, Kaida K, Inoue T, Okada M, Soma T, Ogawa H. Low incidence of human herpesvirus 6 reactivation in unmanipulated HLA-haploidentical related stem cell transplantation with corticosteroid as graft-versus-host disease prophylaxis.

5. 第 37 回日本造血細胞移植学会 2015. 3.5-7, 神戸, Presidential symposium, 小川啓恭、進行期血液腫瘍に対する、低容量 ATG とステロイドを用いた unmanipulated haploidentical RIST

6. 第 37 回日本造血細胞移植学会 2015. 3.5-7, 神戸, Workshop, 海田勝仁、池亀和博、井上貴之、岡田昌也、玉置広哉、相馬俊裕、藤盛好啓、小川啓恭、high tumor burden を有する HLA 半合致移植患者に対する、減量 GVHD 予防の有用性

7. 第 37 回日本造血細胞移植学会 2015.3.5-7, 神戸, 口演, 海田勝仁、池亀和博、井上貴之、岡田昌也、玉置広哉、相馬俊裕、藤盛好啓、小川啓恭、ハプロタイプを共有しない血縁ドナーからの造血幹細胞移植

H. 知的財産権の出願・登録状況

なし。原稿

厚生労働科学研究費補助金（免疫アレルギー疾患等実用化研究事業）
分担研究報告書

「新たな造血幹細胞移植法の開発：生着効率の向上を目指して」に関する研究

研究分担者　豊嶋　崇徳
北海道大学大学院医学研究科　血液内科学分野　教授

研究要旨
移植後シクロホスファミドを用いたHLA半合致末梢血幹細胞移植後の生着不全3例を対象に拒絶メカニズムを考察した。3症例はいずれも複数回HLA不適合移植後であり、不適合HLAを認識する前回移植ドナーのGVHD reaction担当T細胞が、今回の移植片に対してHVG reactionを起こした可能性が考えられた。

A．研究目的

近年、移植後シクロホスファミド(posttarnsplantation cyclophosphamide: PTCy)を用いたHLA半合致移植の有用性が報告されている。この移植法はGVHDの制御に優れ、非再発死亡割合が低いことが利点であるが、骨髄を用いた場合には10-15%程度の生着不全となることが問題点の一つである。今回我々は生着の点からは有利である可能性のある末梢血幹細胞を用いてPTCyを用いたHLA半合致移植後を行い、生着率および生着不全例に関する検討を行った。

B．研究方法

移植前処置はJohns Hopkinsの原法であるFludarabine (30mg/m2×5日)、Cyclophosphamide (14.5mg/kg×2日)、TBI (2Gy)にBusuflfan (3.2mg/kg×2日)を追加した強度減弱前処置を用いた。GVHD予防法は移植後Cyclophosphamide (50mg/kg, day3,4)、Tacrolimus (day5-)、MMF (day5-60)により行った。

C．研究結果

2013年5月より2014年4月までに35例に対してPTCyを用いたHLA半合致位末梢血幹細胞移植を行った。年齢中央値は48歳(21-65歳)、男性22例、女性9例、疾患はAMLが17例(54.8%)、ALL/LBLが8例(25.8%)、MDSが3例(9.7%)、CMMoLが1例(3.2%)、NHLが2例(6.5%)であった。移植時病期は19例(61.3%)が非寛解、また13例(41.9%)は同種移植の既往を有していた。好中球生着は31例中27例(87.1%)に認めれ、1例が生着前感染症死亡、3例が一次生着不全であった。

3例の生着不全例はそれぞれ20代女性、急性骨髄性白血病、3回目の同種移植施行例、CD34: 4.0x10^6/kg、CD3: 0.58x10^6/kg、20代男性、急性リンパ性白血病、3回目の同種移植施行例、CD34: 10.54x10^6/kg、CD3: 2.06x10^6/kg、30代男性、急性リンパ性白血病、2回目の同種移植施行例、CD34: 2.02x10^6/kg、CD3: 2.51x10^6/kgであった。3症例はいずれも複数回HLA不適合移植後であり、前回ドナーとのHVG方向不適合はそれぞれ5座、7座、4座であり、前回移植時のGVH方向の不適合alleleを含んでいた。不適合HLAを認識する前回移植ドナーのGVHD reaction担当T細胞が、今回の移植片に対してHVG reactionを起こした可能性が考えられた。

D．考察

PTCyを用いたHLA半合致移植では免疫抑制剤が投与されない状況下に移植片が輸注されるため、前処置強度が弱くHostのリンパ球の抑制が不十分な場合には、HVG reactionの影響が強くでている可能性がある。

E．結論

複数回HLA不適合移植を行う場合には前回移植ドナーとのHLA適合度も考慮したドナー選択を行う必要がある。

F．健康危険情報

特になし

G．研究発表

1. 論文発表

英文雑誌

1. Nakasone H, Fukuda T, Kanda J, Mori T, Yano S, Kobayashi T, Miyamura K, Eto T, Kanamori H, Iwato K, Uchida N, Mori S, Nagamura-Inoue T, Ichinohe T, Atsuta Y, **Teshima T**, Murata M :

Impact of conditioning intensity and TBI on acute GVHD after hematopoietic cell transplantation.
Bone Marrow Transplant. 2014 Dec 22. [Epub ahead of print]

2. Koyama M, Hashimoto D, Nagafuji K, Eto T, Ohno Y, Aoyama K, Iwasaki H, Miyamoto T, Hill GR, Akashi K, **Teshima T**: Expansion of donor-reactive host T cells in primary graft failure after allogeneic hematopoietic SCT following reduced-intensity conditioning.
Bone Marrow Transplant
2014,49(1):110-115

3. Sugiyama H, Maeda Y, Nishimori H, Yamasuji Y, Matsuoka KI, Fujii N, Kondo E, Shinagawa K, Tanaka T, Takeuchi K, **Teshima T**, Tanimoto M: Mammalian target of rapamycin inhibitors permit regulatory T cell reconstitution and inhibit experimental chronic graft-versus-host disease.
Biol Blood Marrow Transplant
2014,20(2):183-191

4. Shono Y, Shiratori S, Kosugi-Kanaya M, Ueha S, Sugita J, Shigematsu A, Kondo T, Hashimoto D, Fujimoto K, Endo T, Nishio M, Hashino S, Matsuno Y, Matsushima K, Tanaka J, Imamura M, **Teshima T**: Bone marrow graft-versus-host disease: evaluation of its clinical impact on disrupted hematopoiesis after allogeneic hematopoietic stem cell transplantation.
Biol Blood Marrow Transplant
2014,20(4):495-500

5. Shiratori S, Wakasa K, Okada K, Sugita J, Akizawa K, Shigematsu A, Hashimoto D, Fujimoto K, Endo T, Kondo T, Shimizu C, Hashino S, **Teshima T**:Stenotrophomonas maltophilia infection during allogeneic hematopoietic stem cell transplantation: a single-center experience.
Clin Transplant 2014,28(6):656-661

6. Shigematsu A, Kobayashi N, Yasui H, Shindo M, Kakinoki Y, Koda K, Iyama S, Kuroda H, Tsutsumi Y, Imamura M, **Teshima T**:High level of serum soluble interleukin-2 Receptor at Transplantation Predicts Poor Outcome of Allogeneic Stem Cell Transplantation for Adult T Cell Leukemia.
Biol Blood Marrow Transplant
2014,20(6):801-805

7. Iwasaki J, Kondo T, Darmanin S, Ibata M, Onozawa M, Hashimoto D, Sakamoto N, **Teshima T** : FIP1L1 presence in FIP1L1-RARA or FIP1L1-PDGFRA differentially contributes to the pathogenesis of distinct types of leukemia.
Ann Hematol 2014,93(9):1473-1481

8. Takashima S, Eto T, Shiratsuchi M, Hidaka M, Mori Y, Kato K, Kamezaki K, Oku S, Henzan H, Takase K, Matsushima T, Takenaka K, Iwasaki H, Miyamoto T, Akashi K, **Teshima T** :
The use of oral beclomethasone dipropionate in the treatment of gastrointestinal graft-versus-host disease: the experience of the Fukuoka blood and marrow transplantation (BMT) group.
Intern Med 2014,53(12):1315-1320

9. Takahata M, Hashino S, Onozawa M, Shigematsu A, Sugita J, Fujimoto K, Endo T, Kondo T, Tanaka J, Imamura M, **Teshima T** :Hepatitis B virus (HBV) reverse seroconversion (RS) can be prevented even in non-responders to hepatitis B vaccine after allogeneic stem cell transplantation: long-term analysis of intervention in RS with vaccine for patients with previous HBV infection.
Transpl Infect Dis 2014,16(5):797-801

10. Arai S, Arora M, Wang T, Spellman SR, He W, Couriel DR, Urbano-Ispizua A, Cutler CS, Bacigalupo AA, Battiwalla M, Flowers ME, Juckett MB, Lee SJ, Loren AW, Klumpp TR, Prockup SE, Ringdén OT, Savani BN, Socié G, Schultz KR, Spitzer T, **Teshima T**, Bredeson CN, Jacobsohn DA, Hayashi RJ, Drobyski WR, Frangoul HA, Akpek G, Ho VT, Lewis VA, Gale RP, Koreth J, Chao NJ, Aljurf MD, Cooper BW, Laughlin MJ, Hsu JW, Hematti P, Verdonck LF, Solh MM, Norkin M, Reddy V, Martino R, Gadalla S, Goldberg JD, McCarthy PL, Pérez-Simón JA, Khera N, Lewis ID, Atsuta Y, Olsson RF, Saber W, Waller EK, Blaise D, Pidala JA, Martin PJ, Satwani P, Bornhäuser M, Inamoto Y, Weisdorf DJ, Horowitz MM, Pavletic SZ; Graft-vs-Host Disease Working Committee of the CIBMTR :
Increasing incidence of chronic graft-versus-host disease in allogeneic transplantation - A Report from CIBMTR.

Biol Blood Marrow Transplant. 2014 Oct 30. [Epub ahead of print]

11. Hayase E, Fujimoto K, Mitsuhashi T, Hatanaka Y, Yoshida M, Takemura R, Iwasaki J, Shiratori S, Sugita J, Kondo T, Tanaka J, Imamura M, Matsuno Y, **Teshima T**:
Epstein-barr virus-associated smooth muscle tumors after bone marrow transplantation.
Transplantation 2014,97(1):e1-3.

12. **Teshima T** : JAK inhibitors: a home run for GVHD patients?
Blood 2014,123(24):3691-3693

和文雑誌

1. 杉田純一、**豊嶋崇徳**:
Graft-versus-host disease 制御.
臨床血液 55 (2): 170-176, 2014.

2. 杉田純一、小杉瑞葉、**豊嶋崇徳**： 移植後シクロホスファミドを用いた HLA 半合致移植の現状と課題.
日本造血細胞移植学会雑誌
2015,4(1): 9-22

2. 学会発表

1. **豊嶋崇徳** .造血幹細胞移植：HLA バリアを超えて.第 62 回日本輸血・細胞治療学会総会. 2014 年 5 月 15 日. 奈良.

H. 知的財産権の出願・登録状況:

1. 特許取得　　なし
2. 実用新案登録　　なし
3. その他　　なし

厚生労働科学研究費補助金（免疫アレルギー疾患等実用化研究事業）
分担研究報告書

同種造血幹細胞移植後合併症における HMGB1-RAGE 系の関与の検討

研究分担者　前田嘉信　岡山大学病院血液・腫瘍内科　講師

研究要旨　同種造血幹細胞移植後の合併症の克服は、移植成績を向上させる上で重要である。移植後早期に起こる生体内の変化“danger signal”は、その後の移植合併症を誘発させる可能性がある。“danger signal”として、IL-1 や TNF-a などの炎症性サイトカインとともに LPS などの微生物特有の分子群 PAMP (Pathogen-associated molecular pattern ; 病原体関連分子パターン)の役割が明らかにされている。加えて“danger signal”には、外的要因（微生物）としての PAMP に対し、内的要因(細胞障害など)の分子群は DAMP (Damage associated molecular pattern ; ダメージ関連分子パターン）がある。High-mobility group box 1 protein (HMGB-1)は、免疫担当細胞から能動的に細胞外に分泌、または細胞死に伴って受動的に細胞外へ放出さる。受容体としては、receptor for advanced glycation endproducts (RAGE)が知られている。今回、我々はマウスモデルを使って DAMP である HMGB1-RAGE 系と同種造血幹細胞移植後合併症の関連について検討した。その結果、同種移植後には HMGB1 濃度が上昇すること、RAGE を欠損したホストでは GVHD の重症度が異なることが明らかとなった。さらに抗 HMGB1 抗体投与により急性 GVHD の減弱及び生存率の低下を認めた。以上から GVHD における HMGB1-RAGE 系の関与が明らかとなり、治療標的となる可能性が示唆された。

A. 研究目的

同種造血幹細胞移植は、白血病などの悪性疾患に対する根治的治療として確立しているが、致死的合併症である移植片対宿主病（GVHD）は今日なお克服すべき課題である。移植後早期に起こる生体内の変化“danger signal”は、その後の移植合併症を誘発させる可能性がある。今回、我々は、内的要因(細胞障害など)の分子群 DAM である High-mobility group box 1 protein (HMGB-1)に注目し、その受容体 receptor for advanced glycation endproducts (RAGE)と HMGB-1 の同種造血幹細胞移植後合併症における役割を明らかにすることを目的とした。

B. 研究方法

ドナーに B6、ホストに BALB/c を使ったマウス GVHD モデルを作成した。また、HMGB-1 の受容体である RAGE を欠損した RAGE KO マウスをレシピエントに使用した。骨髄幹細胞（T 細胞除去した BM $5x10^6$）と　脾臓から採取した細胞（$5x10^6$）を 13Gy 照射したマウスに移植。急性 GVHD は臨床的 GVHD スコアに加え病理スコアにて評価した。血清中の HMGB-1 は ELISA にて、また、Th 細胞への

影響、細胞内サイトカインをFACSにて解析した。さらに抗HMGB1抗体投与により急性GVHD及び生存率にどのような影響があるかと検討した。

本実験計画は岡山大学実験動物実験委員会に承認済みである。すべての実験動物は動物愛護の観点から、計画的にできるだけ少ない個体数での実験とした。

C. 研究結果

まず、血清中のHMGB-1が移植後の障害により血中に放出されるかを 移植後6時間、24時間、7日目、14日目、21日目と経時的に測定した。同種移植後7日目には他の群に比べ、有意差をもってHMGB-1が上昇しており、免疫反応による組織障害を反映したと考えられた（図1）。

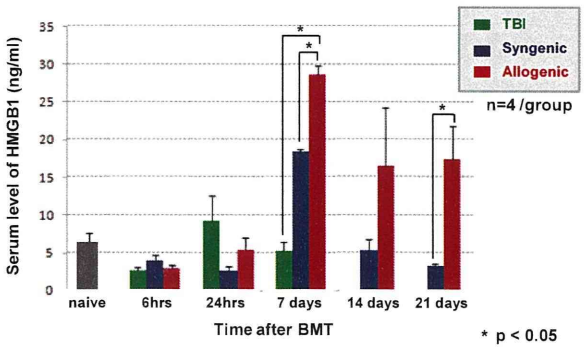

図1 血清HMGB-1濃度

次に、HMGB-1の受容体であるRAGEを欠損したRAGE KOマウスをレシピエントに使用し急性GVHDの発症を野生型WTと比較した。

RAGE KOマウス群では、移植後7-10日の1週間前後で多くが早期死亡を認めWTと比較しても有意に生存率は低い傾向を示した。GVHDスコア、体重減少と合わせてKO群でWTより強い同種免疫反応が生じている可能性があると考えられた。

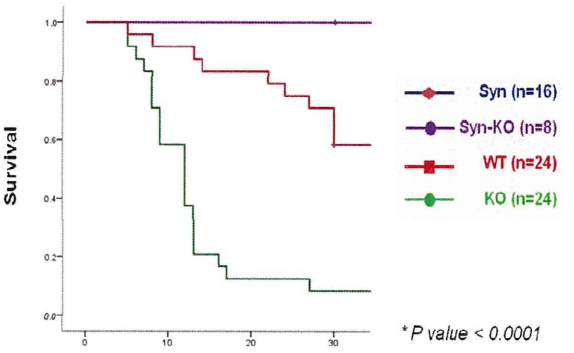

さらに抗HMGB1抗体投与により急性GVHDの減弱及び生存率の低下を認めた。

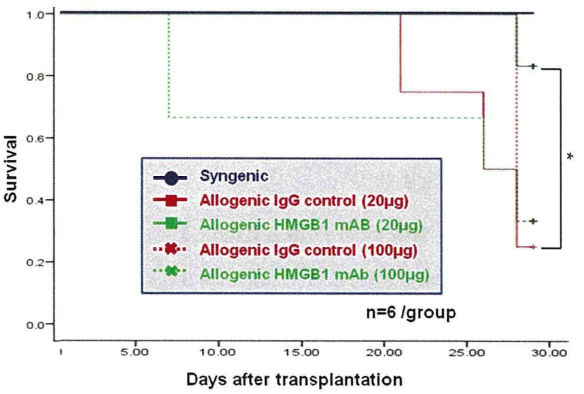

D. 考察

同種移植後7日目には有意差をもってHMGB-1が上昇した。また、受容体を欠損したRAGE KOマウスをレシピエントに使用した場合に急性GVHDの重症度に差を認め、以上からHMGB-1・RAGEの系がGVHDに関与している可能性が示唆された。

E. 結論

HMGB-1 ・RAGE の系が GVHD に関与している可能性が示唆され、今後詳細なメカニズムと治療標的となり得るかと検討していく必要がある。

F. 健康危険情報

特になし。

G.研究発表

1. 論文発表

1) Okamoto S, Fujiwara H, Nishimori H, Matsuoka K, Fujii N, Kondo E, Tanaka T, Yoshimura A, Tanimoto M, Maeda Y. Anti-IL-12/23 p40 antibody attenuates experimental chronic graft versus host disease via suppression of IFN-γ/IL-17-producing cells. **J Immunol**. 2015 in press

2) Sugiyama H, Maeda Y, Nishimori H, Yamasuji Y, Matsuoka K, Fujii N, Kondo E, Shinagawa K, Tanaka T, Takeuchi K, Teshima T, and Tanimoto M. mTOR inhibitors permit regulatory T cell reconstitution and inhibit chronic GVHD. **Biol Blood Marrow Transplant**. 2014; 20(2):183-91

2. 学会発表

1) Taiga Kuroi, Sachiyo Okamoto, Kyosuke Saeki, Yujin Kobayashi, Hisakazu Nishimori, Hideaki Fujiwara, Ken-ichi Matsuoka, Nobuharu Fujii, Eisei Kondo, Mitsune Tanimoto, Yoshinobu Maeda Anti-IL-12/23 p40 Antibody Attenuates Chronic Graft Versus Host Disease Via Suppression of IFN-γ/IL-17 -Producing Cells American Society of Hematology 56th Annual Meeting, San Francisco December 5, 2014

2) Fujiwara H, Maeda Y, Kobayashi K, Nishimori H, Nishinohara M, Okamoto S, Matsuoka K, Kondo E, Fujii N, Shinagawa K, Tanimoto M. PD-1 pathway of donors and recipients modulate chronic graft -versus-host disease through Th1 and Th17 in mouse model. 日本造血幹細胞移植学会 2014 3/7-9 沖縄

H.知的財産権の出願・登録状況（予定を含む。）

1. 特許取得

特になし。

2. 実用新案登録

特になし。

3. その他

特になし

Ⅲ．研究成果の刊行に関する一覧表

研究成果の刊行に関する一覧表

発表者氏名	論文タイトル名	発表誌名	巻号	ページ	出版年
Watanabe K, Terakura S, Martens AC, van Meerten T, Uchiyama S, Imai M, Sakemura R, Goto T, Hanajiri R, Imahashi N, Shimada K, Tomita A, Kiyoi H, Nishida T, Naoe T, Murata M.	Target antigen density governs the efficacy of anti-CD20-CD28-CD3 ζ chimeric antigen receptor-modified effector CD8+ T cells.	*J Immunol.*	194(3)	911-920	2015
Kaida K, Ikegame K, Ikemoto J, Murata R, Irie R, Yoshihara S, Ishii S, Okada M, Inoue T, Tamaki H, Soma T, Fujimori Y, Kai S, Ogawa H.	Soluble interleukin-2 receptor level on day 7 as a predictor of graft-versus-host disease after HLA-haploidentical stem cell transplantation using reduced intensity conditioning.	*Int J Hematol.*	99(4)	463-70	2014
Shono Y, Shiratori S, Kosugi-Kanaya M, Ueha S, Sugita J, Shigematsu A, Kondo T, Hashimoto D, Fujimoto K, Endo T, Nishio M, Hashino S, Matsuno Y, Matsushima K, Tanaka J, Imamura M, Teshima T.	Bone marrow graft-versus-host disease: evaluation of its clinical impact on disrupted hematopoiesis after allogeneic hematopoietic stem cell transplantation.	*Biol Blood Marrow Transplant.*	20(4)	495-500	2014
Fujiwara H, Maeda Y, Kobayashi K, Nishimori H, Matsuoka K, Fujii N, Kondo E, Tanaka T, Chen L, Azuma M, Yagita H, Tanimoto M.	Programmed death-1 pathway in host tissues ameliorates Th17/Th1-mediated experimental chronic graft-versus-host disease.	*J Immunol.*	193(5)	2565-73	2014
Okamoto S, Fujiwara H, Nishimori H, Matsuoka K, Fujii N, Kondo E, Tanaka T, Yoshimura A, Tanimoto M, Maeda Y.	Anti-IL-12/23 p40 antibody attenuates experimental chronic graft versus host disease via suppression of IFN-γ/IL-17-producing cells.	*J Immunol.*	194(3)	1357-63	2015

Ⅳ. 研究成果の刊行物・別刷

Target Antigen Density Governs the Efficacy of Anti–CD20-CD28-CD3 ζ Chimeric Antigen Receptor–Modified Effector CD8$^+$ T Cells

Keisuke Watanabe,*,[1] Seitaro Terakura,*,[1] Anton C. Martens,[†,‡] Tom van Meerten,[§] Susumu Uchiyama,[¶] Misa Imai,[‖] Reona Sakemura,* Tatsunori Goto,* Ryo Hanajiri,* Nobuhiko Imahashi,* Kazuyuki Shimada,*,[#] Akihiro Tomita,* Hitoshi Kiyoi,* Tetsuya Nishida,* Tomoki Naoe,*, and Makoto Murata***

The effectiveness of chimeric Ag receptor (CAR)–transduced T (CAR-T) cells has been attributed to supraphysiological signaling through CARs. Second- and later-generation CARs simultaneously transmit costimulatory signals with CD3ζ signals upon ligation, but may lead to severe adverse effects owing to the recognition of minimal Ag expression outside the target tumor. Currently, the threshold target Ag density for CAR-T cell lysis and further activation, including cytokine production, has not yet been investigated in detail. Therefore, we determined the threshold target Ag density required to induce CAR-T cell responses using novel anti-CD20 CAR-T cells with a CD28 intracellular domain and a CD20-transduced CEM cell model. The newly developed CD20CAR–T cells demonstrated Ag-specific lysis and cytokine secretion, which was a reasonable level as a second-generation CAR. For lytic activity, the threshold Ag density was determined to be ~200 molecules per target cell, whereas the Ag density required for cytokine production of CAR-T cells was ~10-fold higher, at a few thousand per target cell. CD20CAR–T cells responded efficiently to CD20-downregulated lymphoma and leukemia targets, including rituximab- or ofatumumab-refractory primary chronic lymphocytic leukemia cells. Despite the potential influence of the structure, localization, and binding affinity of the CAR/Ag, the threshold determined may be used for target Ag selection. An Ag density below the threshold may not result in adverse effects, whereas that above the threshold may be sufficient for practical effectiveness. CD20CAR–T cells also demonstrated significant lytic activity against CD20-downregulated tumor cells and may exhibit effectiveness for CD20-positive lymphoid malignancies. *The Journal of Immunology*, **2015, 194: 911–920.**

Chimeric Ag receptor (CAR)–transduced T (CAR-T) cell therapy is an emerging therapeutic strategy for refractory acute lymphoblastic leukemia (ALL) and chronic lymphocytic leukemia (CLL) (1, 2). Second- and later-generation CARs generally consist of a single-chain variable fragment (scFv) from a mAb fused to the signaling domain of CD3ζ, and contain one or two costimulatory endodomains, respectively (3–5). This technology has two main potential benefits over TCR gene insertion. One is that Ag recognition by CAR is independent of HLA, meaning that CAR therapy can be used to treat all Ag-positive patients regardless of their HLA. The other is that once CARs ligate to target molecules, full activation signals, including costimuli such as CD28 or 4-1BB, are transmitted to CAR-T cells (3–5). A superior effector function and proliferation following activation have been reported in second- and third-generation CAR-T cells (6–9).

In contrast, CAR-T cells may induce adverse effects by recognizing low expression levels of the target Ag in an off-target organ. This activity has been referred to as the "on-target/off-tumor effect." A serious adverse event induced by CAR-T cells, which recognize very low expression levels of ERBB2 on lung epithelial cells, was reported with CAR therapy targeting ERBB2 based on trastuzumab (Herceptin) (10). Although ERBB2 is expressed at low levels in various normal tissues, including lung, the anti-ERBB2 humanized mAb trastuzumab has been used safely in clinical settings (11), indicating that ERBB2 expression levels on lung cells are negligible in terms of trastuzumab therapy (12). However, ERBB2–CAR-T cells induce significant Ag-specific responses against this low expression of ERBB2 (10, 11). Therefore, selection of a target Ag is critical for both efficacy and avoiding adverse effects. TCRs recognize very low numbers of peptide/HLA complexes, whereas a relatively high number of target molecules are required for mAbs to induce cytotoxic activity (13, 14). However, the range of Ag density in which CAR-T

*Department of Hematology and Oncology, Nagoya University Graduate School of Medicine, Nagoya 466-8560, Japan; [†]Department of Hematology, VU University Medical Center Amsterdam, 1007 MB Amsterdam, the Netherlands; [‡]Department of Immunology, University Medical Center Utrecht, 3508 GA Utrecht, the Netherlands; [§]Department of Hematology, University Medical Center Groningen, 9700 RB Groningen, the Netherlands; [¶]Division of Advanced Science and Biotechnology, Graduate School of Engineering, Osaka University, Osaka 565-0871, Japan; [‖]Faculty of Pharmacy, Meijo University, Nagoya 468-8503, Japan; [#]Institute for Advanced Research, Nagoya University, Nagoya 464-8601, Japan; and **National Hospital Organization Nagoya Medical Center, Nagoya 460-0001, Japan

[1]K.W. and S.T. contributed equally to this work.

Received for publication September 12, 2014. Accepted for publication November 21, 2014.

This work was supported by grants from the Foundation for Promotion of Cancer Research (Tokyo, Japan; to S.T.), the Japan Society for the Promotion of Science KAKENHI (24790969 to S.T.), the Program to Disseminate Tenure Tracking System (MEXT, Japan; to K.S.), a Grant-in-Aid for Challenging Exploratory Research (23659487 to T. Naoe), and a Health Labor Science Research Grant (H25-Immunology-104 to M.M.).

The online version of this article contains supplemental material.

Address correspondence and reprint requests to Dr. Seitaro Terakura, Department of Hematology and Oncology, Nagoya University Graduate School of Medicine, 65 Tsurumai, Showa-ku, Nagoya, Aichi 466-8560, Japan. E-mail address: tseit@med.nagoya-u.ac.jp

Abbreviations used in this article: ABC, Ab-binding capacity; ADCC, Ab-dependent cellular cytotoxicity; ALL, acute lymphoblastic leukemia; CAR, chimeric Ag receptor; CAR-T, CAR-transduced T (cell); CDC, complement-dependent cytotoxicity; CLL, chronic lymphocytic leukemia; DLBCL, diffuse large B cell lymphoma; FCM, flow cytometry; LCL, EBV-transformed lymphoblastoid cell line; MFI, mean fluorescence intensity; ofa, ofatumumab; sABC, specific Ab binding capacity; scFv, single-chain variable fragment; tEGFR, truncated version of the epidermal growth factor receptor.

www.jimmunol.org/cgi/doi/10.4049/jimmunol.1402346

cells can recognize and induce cytotoxicity has not been investigated in detail. Furthermore, research has not yet clarified the number of Ag molecules expressed that could be candidates for targets when expressed at low levels or that should be avoided owing to the on-target/off-tumor effect (15).

CD20 is an activated glycosylated phosphoprotein that is expressed on the surface of B lymphocytes. An anti-CD20 mAb is an effective therapeutic option for various B cell malignancies such as ALL (16), CLL (17), and malignant lymphoma (18, 19). Although combination chemotherapies with rituximab have achieved favorable results in CD20-positive B cell lymphoma patients, acquired resistance to rituximab has become a problem, with a suggested mechanism of reduced expression of CD20 (20–24). Accordingly, a therapeutic option that efficiently eradicates target cells expressing low levels of CD20 that survive rituximab or ofatumumab (ofa) therapy needs to be developed. Therefore, we developed a novel CD20-CAR and investigated the minimum threshold Ag expression level required for lysis of target cells and activation of CAR-T cells. To avoid possible immunological rejection against anti-mouse Abs, we used a humanized anti-CD20 mAb to construct CD20CAR (25). We also assessed its effects against tumor cell lines and primary cells isolated from mAb therapy-refractory, CD20-downregulated B cell tumors (24, 26, 27).

Materials and Methods

Cell lines

K562, CCRF-CEM, SU-DHL-4, SU-DHL-6, SU-DHL-10, Raji, RRBL1, and WILL2 cells were cultured in RPMI 1640 medium. OCI-Ly3 and OCI-Ly10 cells were kind gifts from Dr. K. Takeyama (Dana-Farber Cancer Institute, Boston, MA) and were cultured in IMDM (Sigma-Aldrich, St. Louis, MO). Each type of medium contained 10% FBS, 0.8 mM L-glutamine, and 1% penicillin-streptomycin. RRBL1 and WILL2 cells are cell lines established from a B cell lymphoma patient who exhibited CD20-negative phenotypic changes after repeated chemotherapy with rituximab (26, 27). CD20-transduced CCRF-CEM cell lines (CD20-CEMs) expressing various levels of CD20 were described elsewhere (28). CD20-transduced K562 (CD20-K562) cells were generated by retroviral transduction with the full-length CD20 molecule, as described (29).

Primary B cell tumor cells

Primary B cell tumor cells were obtained from PBMCs (CLL patient) or pleural effusion (lymphoma patient) according to protocols approved by the Institutional Review Board of Nagoya University School of Medicine, and written informed consent was obtained from each patient in accordance with the Declaration of Helsinki.

Quantification of CD20 molecules

CD20 molecules expressed on the surface of CD20-CEMs or other cell lines were quantified using quantitative immunofluorescence indirect assay (QIFIKIT; Dako, Glostrup, Denmark). Briefly, cells were stained with unlabeled anti-CD20 mouse mAb (BD Bioscience, San Jose, CA) or purified mouse IgG-κ (BioLegend, San Diego, CA) as an isotype control. The cells of interest and calibration beads from the kit were then simultaneously labeled with primary mAb, followed by FITC-conjugated goat anti-mouse secondary Ab staining. Labeled cells and calibration beads were analyzed on a flow cytometer, and a standard regression line between fluorescence intensity and Ag density that was expressed as Ab-binding capacity (ABC) in molecules per cell was calculated. Finally, the specific ABC (sABC) was determined by subtracting the background Ab equivalent of the isotype control from ABC (30).

Retroviral vector construction

CD20-binding scFv was constructed based on the reported sequences of the humanized anti-CD20 mAb (OUBM mAb) (25). OUBM mAb exhibits high CD20 binding affinity (K_D, 10.09 nM). H chain and L chain V region segments were linked with an 18-aa linker. scFv was then fused to a human IgG_4 hinge, a CD3-ζ chain, a CD28 costimulatory domain, and a truncated version of the epidermal growth factor receptor (tEGFR) that lacked epidermal growth factor binding and intracellular signaling domains downstream of the self-cleaving T2A sequence (31–33). By inserting the T2A sequence between CD20CAR and tEGFR, the two proteins were coexpressed at equimolar levels from a single transcript. Cell-surface tEGFR was detected using the biotinylated anti-EGFR mAb Erbitux (Bristol-Myers Squibb, New York, NY). The CD20CAR transgene was assembled by overlap extension PCR (34). CD20CAR was inserted into LZRS-pBMN-Z, using HindIII and NotI sites, and the CD20CAR-encoding retrovirus was produced using the Phoenix-Ampho system (Orbigen, San Diego, CA) and concentrated with Retro-X Concentrator (Clontech Laboratories, Mountain View, CA).

Generation, expansion, and selection of CD20CAR-transduced T cells

The PBMCs of a normal donor were isolated by centrifugation of whole blood using Ficoll-Paque (GE Healthcare, Wauwatosa, WI). $CD8^+$ lymphocytes were then purified with immunomagnetic beads (Miltenyi Biotec, Bergisch Gladbach, Germany), activated with anti-CD3/CD28 beads (Invitrogen, Carlsbad, CA), and transduced on day 3 after activation with the recombinant human fibronectin fragment (RetroNectin, Takara Bio, Otsu, Japan) by centrifugation at 2100 rpm for 45 min at 32°C with the retroviral supernatant (multiplicity of infection = 3). T cells were expanded in RPMI 1640 medium containing 10% human serum, 0.8 mM L-glutamine, 1% penicillin-streptomycin, and 0.5 μM 2-ME and supplemented with recombinant human IL-2 to a final concentration of 50 IU/ml. CAR-positive cells were enriched using immunomagnetic selection with biotin-conjugated anti-EGFR mAb and streptavidin beads (Miltenyi Biotec). The transduced T cells were expanded in culture by plating with γ-irradiated EBV-transformed lymphoblastoid cell line (LCL) at a T cell to LCL ratio of 1:7 and supplemented with IL-2 to 50 IU/ml (29).

Flow cytometry

All samples were analyzed with flow cytometry (FCM) on the FACSAria instrument (BD Biosciences), and data were analyzed using FlowJo software (Tree Star, Ashland, OR). Biotinylated Erbitux and streptavidin-PE were used to identify T cells that expressed tEGFR.

[^{51}Cr] release assay and coculture assay

For the [^{51}Cr] release assay, target cells were labeled for 2 h with [^{51}Cr] (PerkinElmer, Waltham, MA), washed twice, dispensed at 2×10^3 cells per well into triplicate cultures in 96-well round-bottom plates, and incubated for 4 h at 37°C with CD20CAR–T cells at various E:T ratios. Percent of specific lysis was calculated using a standard formula [(experimental − spontaneous release)/(maximum load − spontaneous release) × 100 (%)] and expressed as the mean of triplicate samples. Regarding the coculture assay, CEMs were labeled with 0.1 μM CFSE (Invitrogen), washed, and plated with CD20 CAR-T cells at a ratio of 1:1 without IL-2 supplementation. After a 72-h incubation, cells were stained with anti-CD8 mAb and analyzed with FCM. The percentages of CAR-T cells and CEMs within the live cell gates were assessed.

Intracellular cytokine staining and cytokine secretion assay

CD20CAR–T cells and K562 or CCRF-CEM cells that expressed CD20 were mixed at a 1:1 ratio in the presence of brefeldin A (Sigma-Aldrich) and then fixed and permeabilized with Cell Fixation/Permeabilization Kits (BD Biosciences) for intracellular cytokine assay. After fixation, T cells were stained with anti–IFN-γ and anti–CD8-allophycocyanin mAb (BD Biosciences). As a positive control for cytokine production, cells were stimulated with 10 ng/ml PMA and 1 μg/ml ionomycin (Sigma-Aldrich). CD20CAR–T cells and CEMs for the cytokine secretion assay were plated at an E:T ratio of 1:1, and IFN-γ, TNF-α, and IL-2 in the supernatant were measured with ELISA (BD Biosciences) after 16 h of incubation.

CFSE proliferation assay

CD20CAR–T cells were labeled with 0.2 μM CFSE, washed, and then plated with stimulator cells at a ratio of 1:1 without IL-2 supplementation. After a 72- or 96-h incubation, cells were stained with the anti-CD8 mAb, samples were analyzed with FCM, and the division of live $CD8^+$ T cells was assessed with CFSE dye dilution.

Intracellular phospho-flow analysis

CD20CAR–T cells and CD20-CEM cells expressing various levels of CD20 were mixed at a 1:5 ratio, centrifuged briefly, and incubated for various times at 37°C. Cells were then fixed by the addition of BD Cytofix Fixation Buffer at 37°C for 10 min, permeabilized in ice-cold BD Phosflow Perm Buffer III, and incubated on ice for 30 min (BD Biosciences). P-p44/42 MAPK (T202/Y204) or P-Zap-70 (Y319)/SyK(Y532) Rabbit Ab (Cell

Signaling Technology, Danvers, MA) and bovine anti-rabbit IgG-FITC as a secondary Ab (Santa Cruz Biotechnology, Dallas, TX) were used for phospho-specific staining.

Statistical analysis

Differences among results were evaluated with one-way or two-way ANOVA analysis and the Bonferroni test, as appropriate. Differences were considered significant when $p < 0.05$. Statistical analysis was performed using GraphPad Prism Version 5 software.

Results

Generation and functional analysis of CD20CAR-transduced T cells

To develop functional CD20CAR, we constructed CD20CAR consisting of anti–CD20-scFv linked to CD3ζ, a CD28 costimulatory domain, and a tEGFR; $CD8^+$ T cells were then retrovirally transduced with CD20CAR (Fig. 1A). After one course of stimulation and transduction, the expression of CD20CAR generally reached 40–80%. To determine transduction efficiency, CD20CAR and tEGFR were labeled with an anti-Fc Ab and biotinylated Erbitux, respectively. The expression of tEGFR reflected that of CAR on the transduced T cells, and we verified that the expression of CAR and tEGFR was similar after each transduction experiment (Fig. 1B) (32). Transduction efficiency could be monitored with tEGFR with high reproducibility (Fig. 1B, *right panel*). Using intracellular staining, we assessed the ability of CAR-T cells to produce IFN-γ in response to CD20. Stimulation with CD20-K562 cells induced robust production of IFN-γ, whereas mock-transduced K562 cells did not (Fig. 1C). These results demonstrated that CD20CAR–T cells recognized CD20 in an Ag-specific manner. After the transduction culture, CD20CAR-positive cells were enriched to a purity of >95% with biotinylated Erbitux and anti-biotin immunomagnetic beads (32), expanded by stimulating with a γ-irradiated LCL, and then used for subsequent experiments. The expression of CAR/tEGFR before and after LCL stimulation was sufficiently maintained (Fig. 1D). The ability of CD20CAR–T cells to lyse $CD20^+$ target cells was assessed after one course of transduction and expansion. CD20CAR–T cells specifically lysed CD20-K562 cells (Fig. 1E) in a highly reproducible manner (Fig. 1E, *right panel*). To examine background cytotoxicity, CD19CAR (non–target-specific CAR)–transduced T cells were examined for cytotoxicity against K562 or CD20-K562. Both experiments demonstrated almost the same range of cytotoxicity by the CD20CAR–T cells against K562 as in Fig. 1E. The range of cytotoxicity was 7–11% at an E:T ratio of 10:1 ($n = 4$). Two repeated LCL stimulations caused a log-scale expansion that resulted in 10,000-fold expansion of CD20CAR–T cells (Supplemental Fig. 1). The CD20CAR–T cells almost uniformly demonstrated effector phenotype ($CD28^-$, $CD62L^-$, $CD45RO^+$) after LCL stimulation (data not shown). In all subsequent experiments, $CD20CAR^-$ T cells were selected with tEGFR and expanded with one course of LCL stimulation; thus the transduction level of CD20CAR was uniformly >95% (Fig. 1D).

Quantification of CD20 molecules on the surface of CD20-CEMs and cell lines

Although CAR-T cells very efficiently recognize targets, the range of target molecule expression to which CAR-T cells can respond

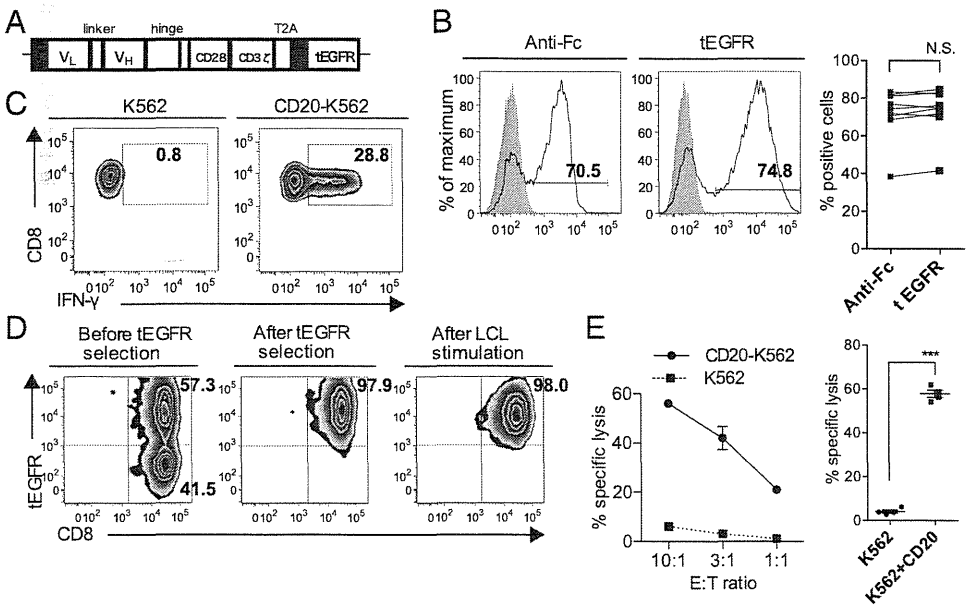

FIGURE 1. Construction, surface expression, and functional analysis of CD20CAR. (**A**) Schematic representation of the CD20CAR construct. CD20CAR consisted of anti-CD20 scFvs linked to CD3ζ, a CD28 costimulatory domain, and tEGFR as a transduction or selection marker via the T2A sequence. Solid black boxes denote the GM-CSF receptor leader sequence. Hinge, a human IgG4 hinge; linker, an 18-aa-long GGGS linker; V_H, H chain variable fragment; V_L, L chain variable fragment. (**B**) Surface expression of CD20CAR and tEGFR after transduction. $CD8^+$ cells were selected and transduced with the CD20CAR-encoding retrovirus supernatant. CD20CAR was stained with the anti-Fc Ab or biotinylated Erbitux, which reflects CAR expression. The surface expression of Fc/tEGFR was assessed on day 8 after one course of retroviral transduction. Gray-shaded histograms show staining of untransduced T cells. Representative flow plots are shown. *Right panel*, Data were pooled from nine independent experiments with T cells from eight donors (NS, paired *t* test). (**C**) Functional analysis of CD20CAR–T cells. On day 9 after transduction, CD20CAR–T cells were stimulated with either CD20-transduced K562 (CD20-K562) or mock-transduced K562 (K562) cells for 4 h at a 1:1 ratio, permeabilized, and then stained for IFN-γ. (**D**) Purity of CD20CAR–T cells before and after tEGFR selection and LCL stimulation. CD20CAR-positive cells were enriched by tEGFR selection and expanded by stimulation with γ-irradiated LCLs at a 1:7 ratio. Representative flow plots of three independent experiments from three donors are shown. (**E**) Cytotoxicity of CD20CAR–T cells. *Left panel*, After one course of expansion, cytotoxicity against either CD20-K562 or K562 cells was assessed at the indicated E:T ratio in the [^{51}Cr] release assay. The means ± SD of triplicate wells are shown. *Right panel*, Data were pooled from four independent experiments with CD20CAR–T cells from four donors (mean and SEM, $***p < 0.0001$, the Student *t* test).

remains unknown (3–5). To assess this range more precisely, the number of CD20 molecules expressed on the cell surface of various cell lines was quantified as the CD20-specific Ab-binding capacity (CD20-sABC) on a per cell basis. We obtained 30 clones of CD20-CEMs expressing various levels of CD20 for use as target cells or stimulators (28). Of these, expression of CD20 by four representative clones was depicted, and the cells were used for several subsequent experiments as stimulators [CD20–very low CEM (VL-CEM) (CD20-mean fluorescence intensity [MFI]: 126/sABC: 240 molecules); CD20–low CEM (L-CEM) (CD20-MFI: 576/sABC: 5320 molecules); CD20–medium CEM (M-CEM) (CD20-MFI: 2396/sABC: 26,900 molecules); and CD20–high CEM (H-CEM) (CD20-MFI: 11,388/sABC: 142,722 molecules)] (Fig. 2A, Table I). The CD20-sABC values were 500,000 molecules for the germinal center B cell–type diffuse large B cell lymphoma (DLBCL)–derived cell lines; SU-DHL-4, -6, and -10, and 100,000 molecules for the non–germinal center B cell–type DLBCL-derived cell lines Ly-3 and -10 (Fig. 2B, Table I). RRBL1 and WILL2 are cell lines established from patients who experienced a relapse in B cell lymphoma with very weak expression of CD20 and who became resistant to rituximab (26, 27). The expression levels of CD20 by RRBL1 and WILL2 cells were 15,632

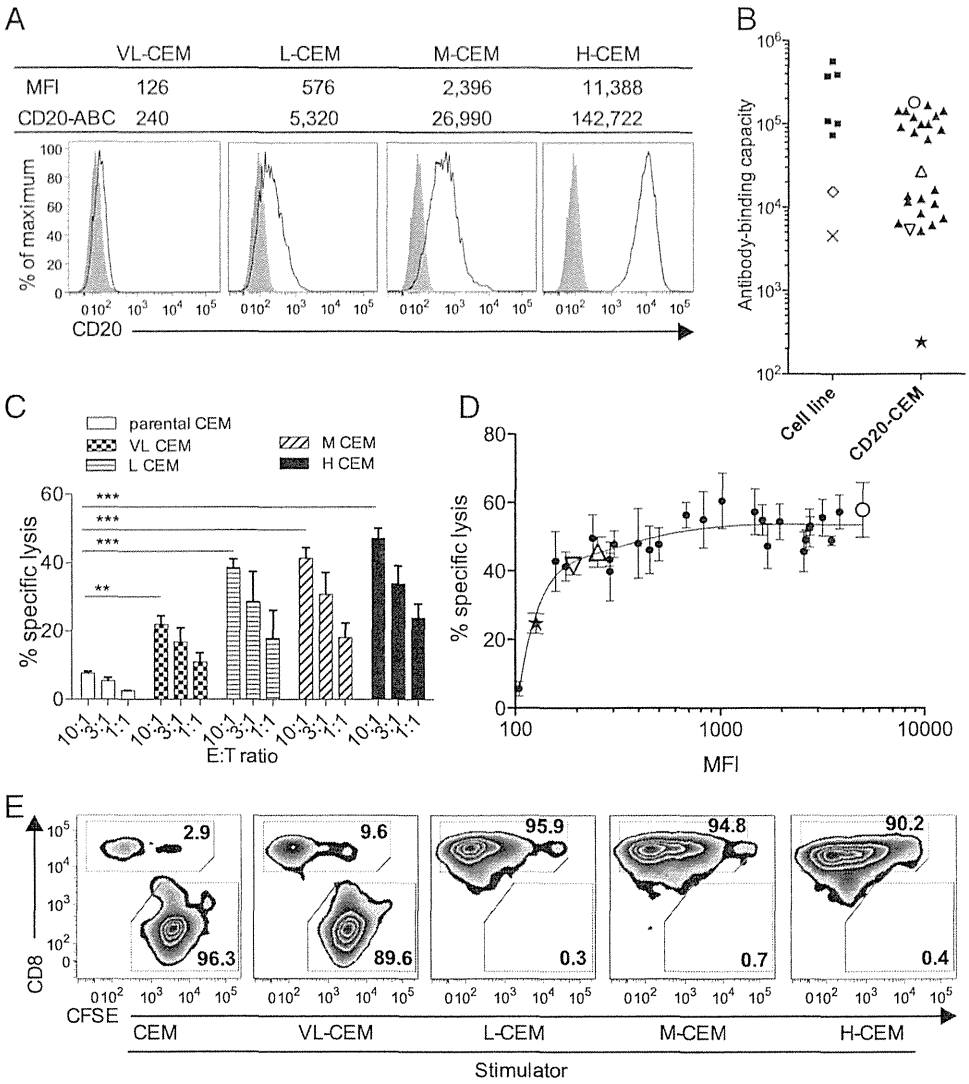

FIGURE 2. Quantification of CD20 molecules on the target cell surface and titration of the CD20 Ag expression level for CD20CAR–T cell cytotoxicity. (**A**) CD20 expression levels of the four representative CD20-CEM cell clones. The table above the histograms shows CD20-MFI and the quantification of CD20 molecules on each cell line as the Ab-binding capacity (CD20-ABC). Gray histograms show CD20 staining of untransduced CEM cells. VL-CEM, CD20-very low CEMs; L-CEM, CD20-low CEMs; M-CEM, CD20-medium CEMs; H-CEM, CD20-high CEMs. (**B**) Quantification of CD20 molecules on the surface of various cell lines. The number of CD20 molecules expressed on the surface of tumor cell lines was plotted in the left column (×, WILL2 cells; ◇, RRBL1 cells; ■, other cell lines). The number on CD20-CEMs is shown in the right column, including the four representative CEMs (★, VL-CEM; ▽, L-CEM; △, M-CEM; ○, H-CEM; ▲, other CD20-CEMs) (B, **D**). CD20-MFI data were analyzed in three independent experiments with similar results. CD20-MFI data in (A), (B), and (D) were collected in different experiments. (**C**) Cytotoxicity of CD20CAR–T cells against the four representative CD20-CEMs. Bars represent the cytotoxicity of CD20CAR–T cells against the four CD20-CEMs or untransduced CEMs (parental CEMs) at the indicated E:T ratios in the [^{51}Cr] release assay. The means ± SD of triplicate wells are shown (**$p < 0.01$, ***$p < 0.0001$, two-way ANOVA analysis). (D) The correlation between the CD20-MFI of CD20-CEMs and the cytotoxicity of CD20CAR–T cells. The cytotoxicity of CD20CAR-T cells against each CD20-CEM cell line was determined as in (C). The cytotoxicity of each CD20-CEM cell line at an E:T ratio of 10:1 was plotted against the CD20-MFI of CD20-CEMs. Data were pooled from four independent experiments with CD20CAR–T cells from four donors (mean and SEM). The solid line represents the fitted curve obtained with the nonlinear regression model using Prism5 software. (**E**) CD20CAR–T cells eradicated CD20-CEMs in coculture assays according to CD20 expression levels. CAR-T cells and CFSE-labeled CEMs were cultured in a 1:1 ratio without IL-2 supplementation for 72 h. The percentage of surviving CAR–T cells and residual CEMs within the live cell gates are shown. Data are representative of three independent experiments using three independent CD20CAR–T cell lines.

Table I. Surface CD20 expression of CD20-CEMs and other tumor cell lines

	MFI	sABC
CEM		
Parental	121	0
#2	9,683	120,208
#3	11,403	142,921
#4	6,905	83,978
#7	7,491	91,567
#19	14,228	180,597
#23	1,293	13,675
#27	11,388	142,722
#29	8,045	98,770
#31	15,550	198,366
#37	845	8,414
#47	1,209	12,680
#71	563	5172
#72	6,494	78,675
#73	8,049	98,822
#76	126	240
#82	641	6,062
#85	9,922	123,353
#94	576	5,320
w6	15,672	200,009
w7	13,180	166,571
w12	1,063	10,960
w40	5,414	64,824
w54	17,930	230,546
w114	1,125	11,689
w127	749	7,303
w132	1,497	16,104
w141	669	6,383
w147	2,396	26,990
w149	11,363	142,390
Tumor cell line		
RRBL1	1,436	15,376
WILL2	510	4,571
DHL-4	33,076	390,664
DHL-6	31,713	371,994
DHL-10	6,983	564,656
Ly-3	6,798	73,049
Ly-10	9,206	100,965
Raji	9,949	108,985

and 4869 molecules per cell, respectively (Fig. 2B, ◇ and ×, respectively). Relative to other cell lines, CD20-CEMs represented a very wide range of CD20 expression, from 240 to 230,546 molecules per cell, which was considered very low to high (Fig. 2B, Table I).

To evaluate the potential influence of costimulation, inhibitory signals, and adhesion molecule, the expression of CD80, CD86, CD54 (ICAM-1), CD58 (leukocyte function–associated molecule-3), and PD-L1 on target tumor cells was investigated. CEM cells demonstrated a tolerogenic phenotype, expressing low levels of CD80 and CD86 and relatively high levels of the inhibitory ligand PD-L1. CD54 was positive in all examined cell lines, whereas CD58 was negative in WILL2 cells (Supplemental Fig. 2) (35).

Determination of the minimum threshold of CD20 expression that CAR-T cells require for recognition and lysis

The level of CD20 Ag expression for rituximab-induced complement-dependent cytotoxicity (CDC) was determined using the same set of CD20-CEMs (28). We performed the rituximab-induced CDC assay and obtained almost the same results using human complement (Supplemental Fig. 3A). As demonstrated previously, Ab-dependent cellular cytotoxicity (ADCC) with rituximab against CD20-CEMs did not show a clear threshold of CD20 expression (data not shown) (28). CD20-CEMs with an MFI <1000 (equivalent to sABC of 10^4) did not induce significant CDC, whereas CD20-CEMs with an MFI of 1000–3000 (equivalent to sABC of 10^4–10^5) did. CD20-CEMs with an MFI >3000 effectively induced cytotoxicity, and maximal CDC was obtained at an MFI >5000 (sABC of 10^5) (Supplemental Fig. 3A). CDC induced by the humanized anti-CD20 mAb OUBM was also examined. OUBM mAb, with which CD20CAR was constructed, induced marked CDC with half-maximum cytotoxicity at a CD20 expression level similar (MFI of 3000) to that of rituximab (MFI of 3000) (Supplemental Fig. 3).

In contrast to the weak CDC caused by rituximab and OUBM mAb, CD20-CEMs were more efficiently lysed by CD20CAR–T cells, with the exception of VL-CEMs, which underwent a significantly lower degree of lysis (Fig. 2C).

To determine the threshold expression level of the CD20 Ag required to induce CAR-T cytotoxicity, we performed a [^{51}Cr] release assay with CD20CAR–T cells against the clones of CD20-CEMs expressing various levels of CD20 (CD20-MFI: 126–6924/CD20-sABC: 240–230,546 molecules). CD20CAR–T cells lysed VL-CEMs, which had the lowest level of CD20 (MFI: 126/sABC: 240 molecules, 22.8 ± 2% lysis). In addition, CD20CAR–T cells induced similar lysis (40–60% lysis) of various CD20-CEMs with higher expression of CD20 (CD20-MFI: 157/CD20-sABC: ≥5172 molecules, E:T ratio of 10:1) (Fig. 2D). CD20CAR–T cells exhibited efficient cytotoxicity against CD20-CEMs with an MFI <1000; at this level, rituximab and OUBM mAb did not induce significant CDC (Supplemental Fig. 3A, 3B, Fig. 2D). Half-maximum cytotoxicity by CD20CAR–T cells was observed at an MFI of ~200–300 (equivalent to sABC of 10^3). Therefore, the minimum threshold number of surface target molecules that CAR-T recognized and lysed was markedly low, at approximately a few hundred molecules.

A coculture assay was performed as a more physiological model. In this assay, CD20CAR–T cells partially, but not completely, eradicated VL-CEMs. Conversely, CAR-T cells completely eradicated L-, M-, and H-CEMs after a 72-h coculture (Fig. 2E).

Intracellular signaling, cytokine production, and cell division after stimulation with the four representative CD20-CEMs

An advantage of CAR-T cell therapy over mAb therapy is that CAR-T cells can become activated and proliferate upon specific stimulation of the target Ag, enabling CAR-T cells to exhibit long-lasting efficacy in vivo (1, 3–5, 9). Although we titrated the threshold Ag density for CAR-T–induced lysis, the threshold for cytotoxicity and full activation, including cytokine production and proliferation, are uncoupled in Ag-specific T cells (36). Thus, we examined the threshold Ag density for CAR-T activation. To define the minimum threshold of CD20 expression that was needed for effective activation and expansion of CAR-T cells, we examined phosphorylation of the signaling molecules ERK and ZAP70 after stimulation with the four representative CD20-CEMs. The CD20-CEMs, except for VL-CEMs, induced similar phosphorylation of ERK (pERK) and ZAP70 in CAR-T cells (Fig. 3A and data not shown). pERK was equally upregulated when CAR-T cells were stimulated with L-, M-, and H-CEMs, but not with VL-CEMs, after 10 min (Fig. 3A). Time-course analysis showed that the pERK MFI responses were almost equal after L-, M-, and H-CEM stimulation, and the peak time was 5–10 min after stimulation. Nevertheless, VL-CEM induced only minimal phosphorylation of ERK in CAR-T cells, similar to that of parental CEMs (Fig. 3A, 3B).

Cytokine production and proliferation were evaluated following different stimuli. Stimulation with VL-CEM did not induce the production of cytokines from CAR-T cells. Conversely, L-, M-, and H-CEMs induced equivalent production of IFN-γ (Fig. 3C–E), IL-2 (Fig. 3F, 3G), and TNF-α (Fig. 3H). IL-2 production after H-CEM

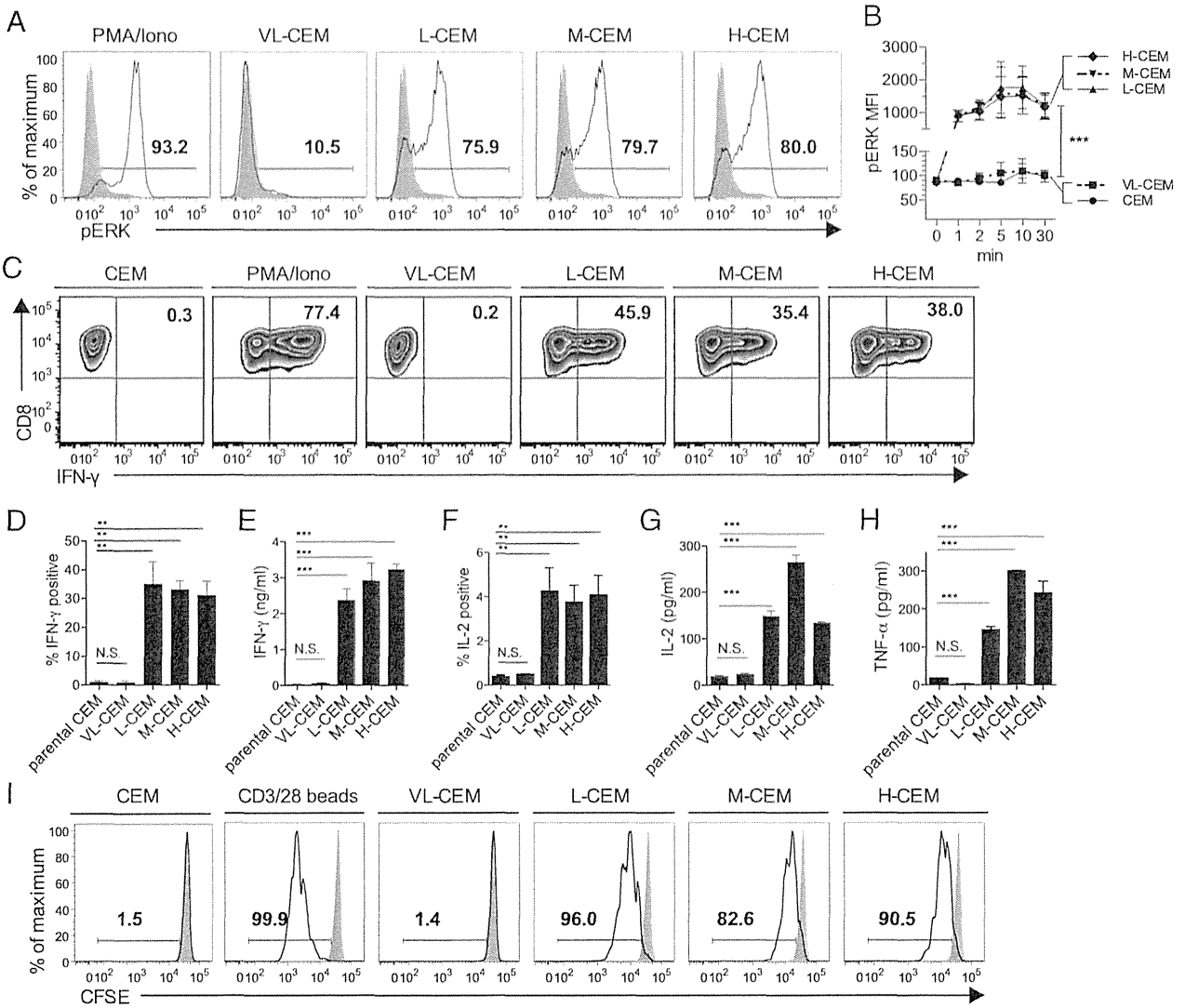

FIGURE 3. Titration of the threshold of CD20 expression for CD20CAR–T cell activation upon stimulation. (**A**) Phosphorylation of a distal signaling molecule, ERK (pERK). CD20CAR–T cells were stimulated with the four representative CD20-CEMs, untransduced CEMs at a responder to stimulator ratio of 1:5, or PMA/ionomycin (Iono) for 10 min, and were then fixed, permeabilized, and stained with pERK-specific Ab. Gray histograms show data obtained from T cells stimulated with parental CEMs. (**B**) Time-course analysis of pERK. The phosphorylation of ERK in CD20CAR–T cells was analyzed 1, 2, 5, 10, and 30 min after stimulation with the four representative CD20-CEMs or parental CEMs at a 1:5 ratio. MFI of pERK after stimulation is shown. Data were pooled from three independent experiments with CD20CAR–T cells from three donors. Means and SEM are shown ($***p < 0.0001$, two-way ANOVA analysis). (**C**) IFN-γ production after stimulation. CD20CAR–T cells were stimulated with the four representative CD20-CEMs, parental CEMs at a 1:1 ratio, or PMA/Iono for 4 h, and were then permeabilized and stained for IFN-γ. (**D** and **F**) The percentages of T cells that stained positive for IFN-γ and IL-2, respectively, are shown. Data were pooled from three independent experiments with CD20CAR–T cells from three donors (mean and SEM, $**p < 0.01$). The secretion of (**E**) IFN-γ, (**G**) IL-2, and (**H**) TNF-α upon CD20-CEM stimulation. CD20CAR–T cells were stimulated with the indicated CEMs at a 1:1 ratio, and culture supernatants were harvested at 16 h and analyzed with ELISA (mean and SEM, $***p < 0.001$, one-way ANOVA). (**I**) Division of CD20CAR–T cells upon CD20 ligation. CD20CAR–T cells were labeled with CFSE and stimulated with CD20-CEMs, untransduced CEMs, or anti-CD3/28 beads at a 1:1 ratio, and the CFSE staining intensity was then analyzed with FCM 96 h after stimulation. Gray histograms show data of nonstimulated CD20CAR–T cells. Data are representative of at least three independent experiments with CD20CAR–T cells from three donors (A, C, and I).

stimulation was approximately half that after M-CEM stimulation in repeated experiments ($n = 3$). Because we observed no significant difference in intracellular IL-2 production (Fig. 3F), the low IL-2 concentration after H-CEM stimulation may have reflected an increase in cytokine consumption. Regarding proliferation, VL-CEM did not induce cell division of CAR-T cells, whereas other CEMs induced efficient cell division 72 and 96 h after stimulation (Fig. 3I and data not shown). The kinetics of CD20CAR–T cell division increased with higher CD20 expression on CD20-CEMs, but the percentages of proliferating cells were equivalent among L-, M-, and H-CEM stimulation (Fig. 3I). The kinetics of division appeared to be partly dependent on target Ag density (Fig. 3I).

Taken together, the minimum threshold required to induce activation and proliferation of CAR-T cells was between the levels expressed by VL-CEMs and L-CEMs. This threshold was very low: less than the CD20 expression level of L-CEMs (CD20-MFI: 576/CD20-sABC: 5320). CD20 expression above the threshold significantly activated CAR-T cells.

Effects on CD20^{lo} cell lines and CD20^{lo} primary tumor cells isolated from patients with rituximab-refractory B cell lymphoma

Because we demonstrated that CD20CAR–T cells recognized markedly low expression of CD20, we examined the effectiveness of

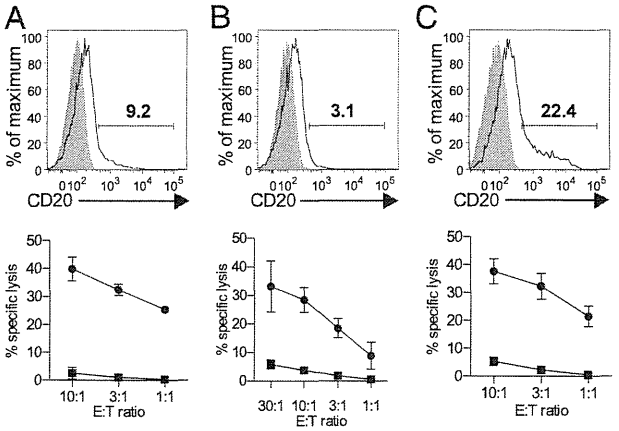

FIGURE 4. Cytotoxicity of CD20CAR–T cells against CD20-downregulated tumor cell lines and primary lymphoma cells. (**A** and **B**) CD20 expression and cytotoxicity by CD20CAR–T cells against CD20-downregulated tumor cell lines RRBL1 and WILL2, respectively. (**C**) CD20 expression and cytotoxicity by CD20CAR–T cells against primary tumor cells isolated from the pleural effusion of a patient with rituximab-refractory B cell lymphoma. Throughout the figure, *upper panels* show CD20 staining (solid line), isotype control staining (gray shaded), and percentages of CD20-positive fractions. *Lower panels* show the cytotoxicity by CD20CAR–T cells against the cell lines at the indicated E:T ratios in the [^{51}Cr] release assay. The means ± SEM of three independent experiments with CD20CAR–T cells from three donors are shown. • and ■ denote cytotoxicity by CD20CAR-T and untransduced T cells, respectively.

CD20CAR–T cell therapy against CD20^{lo} tumor cells. First, the cytotoxicity of CD20CAR–T cells against CD20^{lo} tumor cell lines was investigated. CD20CAR–T cells lysed both CD20^{lo} cell lines, RRBL1 and WILL2, very efficiently (Fig. 2B, 4A, 4B, *lower panel*).

We also evaluated cytotoxicity against CD20^{lo} primary cells from a patient with DLBCL (double-hit lymphoma). The patient exhibited disease recurrence after a full course of R-hyper CVAD (37), and lymphoma cells were obtained from pleural effusion. At the time of relapse, CD20 expression was reduced in most cells, and only ~20% of cells showed low CD20 expression (Fig. 4C, *upper panel*). CD20CAR–T cells efficiently lysed CD20^{lo} primary DLBCL cells. This lytic activity was higher than the percentage of the CD20$^+$ cell fraction, suggesting that CD20CAR–T cells partially lysed the cell fraction expressing low levels of CD20 (Fig. 4C, *lower panel*).

CD20CAR–T cells recognized and lysed residual CLL cells after ofa therapy

CLL is a chronic lymphoproliferative disease in which the anti-CD20 mAb is a choice for standard care (38). The expression of CD20 by CLL cells is generally lower than that of other CD20$^+$ lymphoid malignancies such as ALL and lymphoma (39). To compare the potency of CD20 recognition by anti-CD20 mAb, we examined cytotoxicity and cytokine production following stimulation of CD20-downregulated CLL cells. Before starting mAb therapy, the expression of CD20 by CLL cells was intact, and the lytic activity of CD20CAR–T cells was remarkable (Fig. 5A). The patient then became chemorefractory following repeated administration of rituximab (the clinical course of this patient is summarized in Supplemental Fig. 4). In this patient, CLL cells could not be controlled with rituximab-combined chemotherapy. The expression of CD20 by CLL cells decreased, and the MFI showed two peaks: the nearly negative fraction and the CD20 low fraction (Fig. 5B, *upper panel*). However, cytotoxicity by CD20CAR–T cells was maintained (Fig. 5B, *lower panel*). The patient was then treated with the novel anti-CD20 mAb ofa (40). A marked decrease in the number of CLL cells and regression of lymphadenopathy were observed after a single course of ofa, whereas the CD20 very low fraction, which was confirmed to consist of CD5$^+$ CLL cells (data not shown), remained in the peripheral

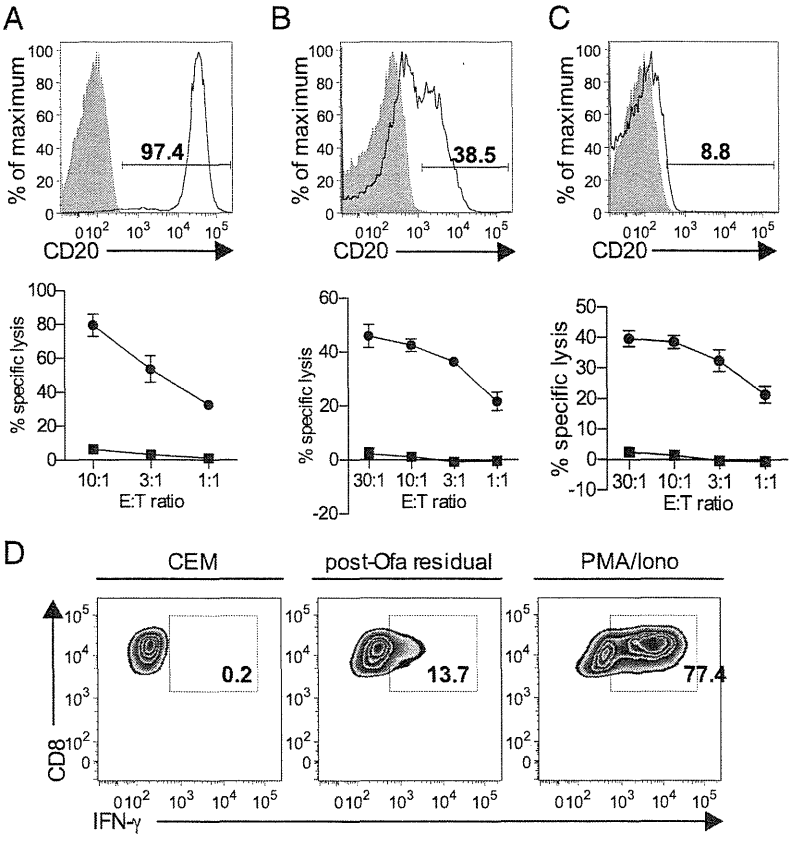

FIGURE 5. Cytotoxicity of CD20CAR–T cells against CD20-downregulated primary CLL cells. (**A–C**) CD20 expression and cytotoxicity against CLL cells isolated from an untreated patient (A), before administration of ofa (preofa) (B), and 14 d after the 10th course of ofa (postofa) (C). CLL cells were isolated from the peripheral blood of a patient with rituximab-refractory CLL. Residual CLL cells after rituximab treatment were isolated from the peripheral blood of a patient at two different time points, pre- and postofa. *Upper panels* show CD20 staining (solid line) and isotype control staining (gray shaded). *Lower panels* show cytotoxicity by CD20CAR–T cells against CLL cells at the indicated E:T ratios in the [^{51}Cr] release assay. Filled circles and squares denote cytotoxicity by CD20CAR-T and untransduced T cells, respectively. The means ± SEM of three independent experiments with CD20CAR–T cells from three donors are shown (A–C). (**D**) Cytokine production by CD20CAR–T cells upon stimulation with postofa CLL cells. CD20CAR–T cells were stimulated with postofa CLL cells, parental CEMs at a 1:1 ratio, or PMA/Iono for 4 h, and were then permeabilized and stained for IFN-γ.

blood. We obtained residual CLL cells from the peripheral blood of the patient after the 10th course of ofa. After ofa treatment, the CD20 relatively low fraction disappeared, and CD20 expression by CLL cells was almost uniformly nearly negative (Fig. 5C, *upper panel*). The residual cells were exposed once to the mAb therapy and survived. Therefore, the CD20 expression level of the residual cells was considered to be below the effective range of rituximab or ofa. In the [^{51}Cr] release assay using these primary CLL cells, CD20CAR–T cells efficiently recognized and lysed not only CLL cells before ofa but also CLL cells after ofa (Fig. 5B, 5C, *lower panel*). With an intracellular IFN-γ assay, after ofa, stimulation of CD20CAR–T cells with CLL cells, which were nearly CD20-negative, induced production of IFN-γ by CD20CAR–T cells (Fig. 5D).

Discussion

In the current study, we generated a novel CD20CAR based on a humanized anti-CD20 mAb (25). CD20CAR–T cells specifically and effectively lysed CD20-positive target cells. The expression of CD20CAR was precisely evaluated using the anti-Fc Ab and biotinylated Erbitux. Although we did not directly evaluate the copy number of the CD20CAR transgene, the variation observed in lytic activity against K562-CD20 cells was very low following tEGFR selection, suggesting that the expression of CD20CAR was similar among the CD20CAR–T cell lines. With cytotoxicity analysis of CD20CAR–T cells against CD20-CEMs expressing various levels of CD20, we first titrated the minimum threshold of CD20 expression that CAR-T cells could recognize and lyse. We demonstrated that CD20CAR–T cells lysed CD20-CEMs with CD20-ABC = 240 molecules, which was the lowest CD20 level in this set. This level was 1000-fold lower than that required to induce CDC with rituximab and OUBM mAb. The difference in cytolytic activity between CDC and CAR should mostly depend on the presence or absence of effector cells. Although CDC and CAR activity is similar against CD20-high CEM cells, CD20CAR–T cells demonstrated far better lytic activity than CDC against CD20-low CEM cells (Fig. 2D, Supplemental Fig. 3). This finding suggested that CAR-T therapy might show better effect in the case of only a limited number of target Ags on the tumor cells. The correlation between CD20-ABC and specific lysis was also represented with a saturation curve, which had a sharp inclination against CD20^{lo} targets. This phenomenon was attributed to CAR technology providing full activation with CD3ζ and the simultaneous costimulation of CD28 (3–6).

We next determined the threshold of CD20 expression that could activate and expand CD20CAR–T cells upon stimulation with the representative CD20-CEMs. Although cytotoxicity analysis revealed that CD20CAR–T cells lysed VL-CEMs, these cells did not induce downstream signaling, production of IFN-γ, or proliferation of CAR–T cells. Stimulation with L-, M-, and H-CEMs (CD20-ABC: ≥5320 molecules) effectively and equally activated CD20CAR–T cells. Taken together, these results indicated that the threshold of CD20 expression for recognition and lysis by CD20CAR–T cells, which we termed the "lytic threshold," was a few hundred molecules, and the threshold required for activation and expansion of CAR-T cells, termed the "activating threshold," was slightly higher, at a few thousand molecules. These results are consistent with previous findings in which the lytic threshold and activating threshold were different in TCR activation (36). Because endogenous T cells such as melanoma-specific T cells and virus-specific T cells require 10–100 epitope molecules per target cell to trigger specific lysis (13), both the lytic threshold and the activating threshold were slightly lower in endogenous T cells compared with CAR-T cells. Obviously, the thresholds are affected by the affinity of the mAb or TCR for the ligand or peptide/HLA complex. In our study, the affinity of the humanized anti-CD20 mAb (OUBM mAb), which was used to construct CD20CAR, was within the same range as that of rituximab (K_D value: OUBM mAb, 10.09 nM; rituximab, 5.35 nM) (25). Using a mAb with this range of affinity, both thresholds of CAR-T cells were close to those of endogenous T cells. Furthermore, CD20CAR–T cells recognized and lysed CD20-downregulated target cells that survived after mAb therapy, indicating that manufacturing a CAR with a mAb may reinforce target recognition more than the mAb itself.

The epitope location of the mAb is another important issue. Ofa exposure before sample collection may account for the apparent CD20 downregulation. However, we confirmed CD20 downregulation using another CD20 mAb, a B9E9 clone in which the epitope location is distinct from that of ofa (23). This confirmation indicated that CD20 downregulation after ofa treatment was not caused by competition between the analytical Ab and ofa. The epitope location targeted by OUBM mAb and ofa partially overlaps, but that of OUBM mAb and rituximab does not (25). Therefore, ofa can theoretically block the ligation of CD20CAR-T but rituximab cannot. We observed that CD20CAR–T cells indeed lysed CD20-downregulated target cells both after rituximab and ofa, suggesting that the potential effect of epitope blocking was minor in the current study.

The results of the current study led us to propose a novel concept for future searches for target Ag in CAR-T therapy. Suitable target Ags for CAR-T cell therapy are considerably different from those for mAb therapy in terms of their expression profiles and levels. Higher expression levels on the surface of tumor cells have been considered in target Ag searches for mAb therapy because off-tumor expression is usually negligible (41). However, for the target of CAR-T cell therapy, off-tumor expression of the target molecules must be strictly negative or at a very low level that is below the lytic threshold, at a few hundred molecules. Otherwise, severe adverse effects could occur as a result of off-tumor effects (10). The target Ag safety in the context of mAb therapy does not necessarily translate into the safety of Ag in the context of markedly more sensitive CAR-T cell therapy (10). Conversely, even if the threshold was below the mAb therapy range, low Ag expression above the activating threshold, such as at a few thousand molecules, could be considered a candidate for the target Ag of CAR-T cell therapy.

Acquired resistance to rituximab has become a problem in the treatment of patients with CD20-positive B cell tumors (20, 23). One suggested mechanism is downregulation of CD20 (20, 22, 26). A total of 15–20% of relapsed patients exhibit CD20 Ag loss, as observed with immunohistochemistry analysis in samples taken at relapse (20, 23). Our CD20CAR–T cells recognized and lysed primary cells isolated from patients with mAb therapy–refractory lymphoma and CLL, although the expression level of CD20 was very low. We also analyzed CD20CAR-T recognition against CD20-downregulated, mAb-refractory CLL in detail (21). The residual cells after CD20 mAb therapy expressed significantly low levels of CD20, and this expression level must have been below the effective range of the mAb in principle. CD20CAR–T cells lysed both postrituximab and postofa residual CLL cells, indicating that CD20CAR–T cells have a greater potential to recognize the target than mAbs. Even residual postofa CLL cells stimulated CD20CAR–T cells, and thus we conclude that the very low expression of CD20 on CLL cells could still efficiently provide stimulation for the further repopulation of CD20CAR–T cells.

In other CAR therapies targeting CD19, several patients were reported to have relapsed despite the completely negative con-